Neuron 52, 619–631, November 22, 2006 ©2006 Elsevier Inc. DOI 10.1016/j.neuron.2006.10.004

In Vivo Imaging Reveals Dendritic Targeting of Laminated Afferents by Zebrafish Retinal Ganglion Cells

Jeff S. Mumm,[1,4,*] Philip R. Williams,[1] Leanne Godinho,[1] Amy Koerber,[1] Andrew J. Pittman,[2] Tobias Roeser,[3] Chi-Bin Chien,[2] Herwig Baier,[3] and Rachel O.L. Wong[1,5,*]

[1] Department of Anatomy & Neurobiology
Washington University School of Medicine
St. Louis, Missouri 63110

[2] Department of Neurobiology and Anatomy
and Brain Institute
University of Utah
Salt Lake City, Utah 84112

[3] Department of Physiology
Programs in Neuroscience, Genetics,
and Developmental Biology
University of California, San Francisco
San Francisco, California 94158

Summary

Targeting of axons and dendrites to particular synaptic laminae is an important mechanism by which precise patterns of neuronal connectivity are established. Although axons target specific laminae during development, dendritic lamination has been thought to occur largely by pruning of inappropriately placed arbors. We discovered by in vivo time-lapse imaging that retinal ganglion cell (RGC) dendrites in zebrafish show growth patterns implicating dendritic targeting as a mechanism for contacting appropriate synaptic partners. Populations of RGCs labeled in transgenic animals establish distinct dendritic strata sequentially, predominantly from the inner to outer retina. Imaging individual cells over successive days confirmed that multistratified RGCs generate strata sequentially, each arbor elaborating within a specific lamina. Simultaneous imaging of RGCs and subpopulations of presynaptic amacrine interneurons revealed that RGC dendrites appear to target amacrine plexuses that had already laminated. Dendritic targeting of prepatterned afferents may thus be a novel mechanism for establishing proper synaptic connectivity.

Introduction

Our understanding of how precise patterns of neuronal connectivity are established during development comes largely from studies of axonal pathfinding and targeting. Initial overgrowth and subsequent elimination of inappropriate axonal projections is a generally accepted model for how synaptic partnerships are established (Luo and O'Leary, 2005). In some instances, however, initial axonal elaborations may be much more precise than previously suspected (Katz and Crowley, 2002). Specific patterns of dendritic growth and elaboration may also be important for ensuring proper wiring between synaptic partners (McAllister, 2000; Wong and Ghosh, 2002; Jan and Jan, 2003). There is in fact evidence for early dendritic targeting in determining the specificity of topographic maps in the *Drosophila* olfactory system (Komiyama and Luo, 2006). However, dendritic targeting as a mechanism by which vertebrate CNS neurons establish proper contact with presynaptic partners has not been fully explored.

Synaptic connections that are arranged into discrete layers or laminae are found in many regions of the central nervous system (CNS). Circuitry organized in this fashion provides a readily assessable system for studying how dendrites and axons target each other during synaptogenesis in the vertebrate CNS (Sanes and Yamagata, 1999). The inner plexiform layer (IPL) of the retina is composed of laminar synaptic connections between retinal ganglion cells (RGCs) and their presynaptic partners, bipolar and amacrine cells (Cajal, 1972; Wässle, 2004; Mumm et al., 2005). Broadly, the IPL is divided into two functionally distinct sublaminae: connections of ON circuits (cells depolarizing in response to increased illumination) and OFF circuits (cells hyperpolarized by light) are localized to the inner and outer halves of the IPL, respectively (Famiglietti and Kolb, 1976). Within the ON and OFF sublaminae are multiple strata, each believed to function as a discrete microcircuit responsible for transmitting a particular set of properties about the visual scene (Lettvin et al., 1959; Roska and Werblin, 2001; Wässle, 2004). Accordingly, the dendritic arbors of RGCs and the terminal arbors of amacrine and bipolar cells arborize within a specific stratum or discrete subsets of strata within the IPL (Cajal, 1972). Thus, determining the cellular strategies retinal neurons adopt to attain laminated arbors will provide insight into how specificity in neuronal connectivity arises.

Past studies in mammals suggested that dendritic segregation into ON and OFF subregions in the IPL is the result of selective elimination of branches from inappropriate regions following an initial stage of overgrowth (Dann et al., 1988; Ramoa et al., 1988; reviewed by Sernagor et al., 2001; Chalupa and Gunhan, 2004; Xu and Tian, 2004). RGC dendritic arbors that eventually come to be monostratified in either the ON or OFF subregions appear to ramify throughout the depth of the IPL during development (Maslim et al., 1986; Bodnarenko et al., 1995, 1999). However, because RGCs comprise many subtypes of cells with different dendritic morphologies and because subtypes cannot be readily distinguished early in development, sampling undefined populations may not reveal variations in how RGC dendrites become laminated.

Here, we used the zebrafish retina as a model system to investigate how dendritic arbors contact appropriate presynaptic partners during development in vivo. The hallmarks of vertebrate retinal development are conserved in zebrafish and occur very rapidly; visual signaling is evident just prior to the start of the third day of

*Correspondence: jeff@luminomics.com (J.S.M.), wongr2@u.washington.edu (R.O.L.W.)
[4] Present address: Luminomics, Inc., St. Louis, Missouri 63104.
[5] Present address: Department of Biological Structure, University of Washington, Seattle, Washington 98195.

development, and visual behaviors, such as the optokinetic response, become evident during the third day of development and are robust by day four (Easter and Nicola, 1996, 1997; Niell and Smith, 2005). Thus, because zebrafish embryos progress rapidly from egg to visually behaving larvae in 5 days and transparency can be maintained during this time, they are ideally suited for in vivo time-lapse imaging of morphological development of the retina. The first RGCs are born between 27–28 hr postfertilization (hpf), followed by cells of the inner nuclear layer 10 hr later (~38 hpf) and then by the photoreceptor layer (~48 hpf; Hu and Easter, 1999). RGC axons leave the retina at 32 hpf and begin to innervate the tectum at 45–48 hpf (Stuermer, 1988; Burrill and Easter, 1995). Differentiation of RGCs is followed closely by that of amacrine cells, and the neurites of these two populations begin to form the IPL by 40 hpf (Kay et al., 2004; Godinho et al., 2005). Conventional synaptic connections within the IPL are evident at 60 hpf, coincident with the first evidence of bipolar cell innervation of the IPL and the appearance of photoreceptor outer segment discs (Schmitt and Dowling, 1999). Photoreceptor ribbon triads form in the outer plexiform layer by 65 hpf, and bipolar ribbon synapses form within the IPL by 70 hpf (Schmitt and Dowling, 1999).

The combined use of noninvasive reporters, such as green fluorescent protein (GFP), and high-resolution confocal microscopy has resulted in insights into the dynamics of neuronal development in zebrafish (Jontes et al., 2000; Kay et al., 2004; Niell et al., 2004; Godinho et al., 2005). Here we have employed transgenic zebrafish lines to visualize RGC dendrites and amacrine neurites simultaneously during circuit formation. In addition, transient mosaic expression of fluorescent reporters allowed us to follow how the dendrites of individual RGCs develop. Collectively, our observations reveal that most zebrafish RGCs precisely target synaptic strata within the IPL while exhibiting diverse dendritic growth and arborization patterns. Moreover, our results implicate amacrine cells as a potential source of lamination cues for their RGC partners.

Results

Stability of RGC Dendritic Terminals Increases upon Stratification

We first examined whether the dendrite dynamics of developing RGCs provide insight into how dendritic lamination occurs in vivo. To visualize individual RGCs, the zebrafish *brn3c* promoter (Xiao et al., 2005) was used to drive mosaic expression of a membrane-targeted yellow fluorescent protein (MYFP) reporter in embryonic and larval zebrafish retinas. This was performed in the background of the *Pax6-DF4:MCFP^{Q01}* transgenic line ("*Q01*"; Godinho et al., 2005) where the majority of retinal cells express membrane-tagged CFP (MCFP). Because CFP is targeted to cellular membranes, synaptic neuropil such as the IPL are brightly labeled in *Q01* fish. Thus, simultaneous dual-color imaging allowed RGC dendritic growth patterns to be correlated directly to their relative depth within the IPL.

We found that RGC dendrites exhibited highly dynamic behaviors prior to evidence of stratification (e.g., at 2.5 days postfertilization, 2.5 dpf). A recording of a cell with an immature dendritic arbor is provided in Figure 1A (see Movie S1 in the Supplemental Data available online). Terminal dendritic branches extended, retracted, and were added or eliminated, within minutes, resulting in no significant net increase in total dendritic length over a 30 min recording period (Figures 1B–1D). Moreover, no evidence of simple linear outgrowth was observed for any single dendrite. Rather, all dendritic termini remained highly motile; no terminus remained within a radius of 1 μm for more than 25 min (Figure 1E). In fact, only about 50% of terminal dendritic branches persisted beyond 30 min (Figure 1F). A spatial distribution plot of stable and transient processes over the 30 min recording period shows no clear correlation between branch persistence and IPL depth (Figure S1). In particular, no evidence of preferential stabilization within strata relevant to the more mature stratification pattern (3.5 dpf, data not shown) was found (Figure S1). Similar dynamic behaviors were evident for all RGC dendrites observed, before they began to stratify (Figures 1F and 1G). In contrast, dendrites became relatively more stable in RGCs with stratified arbors (Figures 1F and 1H; Movie S2). This general pattern of initially exuberant dendritic dynamics followed by increasing stabilization with maturity is similar to in vivo observations in other vertebrate systems (Rajan and Cline, 1998; Wu et al., 1999; Lendvai et al., 2000).

Dendritic Lamination of a Large Subset of RGCs Occurs Sequentially

Because lamination patterns could not be predicted from short recording periods of immature RGCs, we acquired images of RGCs over several days in order to directly visualize how dendritic stratification emerges. To visualize subpopulations of RGCs undergoing dendritic stratification, we crossed a *Brn3c:MGFP* transgenic line to the *Q01* line. Approximately 50% of RGCs express MGFP in the *Brn3c:MGFP* line used (allele *s356t*; Xiao et al., 2005). Thus, in double transgenics, it was possible to determine the location of emerging RGC dendritic strata relative to their depth within the developing IPL.

Time-lapse imaging of *Brn3c:MGFP/Q01* fish revealed that initially, a dense plexus made up predominantly of RGC dendrites formed at the interface between the ganglion cell layer (GCL) and the amacrine cell layer (Figure 2A, 2.5 dpf). Immunolabeling indicated that all RGCs initially arborized in this dendrite-rich plexus, not just the subpopulation labeled in the *Brn3c:MGFP* line (Figures S2A and S2B). At this early stage, a subpopulation of amacrine cells is embedded within the nascent IPL (Schmitt and Dowling, 1999; Godinho et al., 2005). The cell bodies of these amacrine cells appear to form a barrier to RGC dendrite outgrowth (Figure 2A, arrows). Imaging of individual RGCs in the background of a transgenic line in which all amacrines are labeled (*ptf1a:GFP*) confirmed that immature RGC dendrites initially aggregate below the somata of the IPL-embedded amacrine cells. Later, RGC dendrites typically extend around the IPL-embedded amacrine cell bodies to innervate deeper regions of the IPL, and these amacrine cells became displaced to the GCL (Figures S2C and S2D; Godinho et al., 2005).

As development progressed, the IPL expanded along with the rest of the eye, and as RGC dendrites

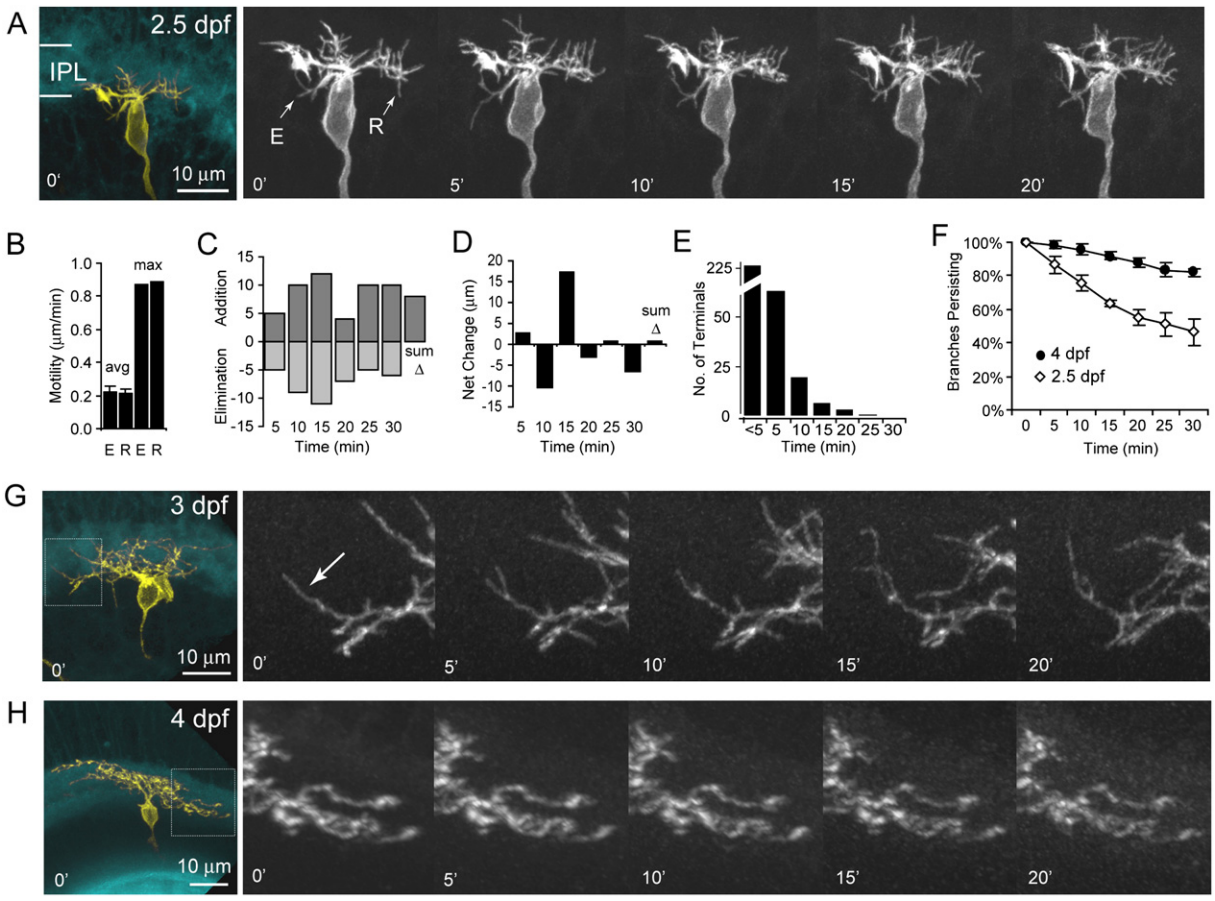

Figure 1. Rapid Time-Lapse Imaging of RGCs Reveals Increasing Stabilization of Dendrites upon Lamination

(A) Isolated immature RGC (MYFP) in the *Q01* background (MCFP). Time-lapse images (5 min intervals) of this cell (grayscale images) show that the dendritic tips are highly exploratory; extensions (E) and retractions (R) are apparent (arrows; Movie S1).

(B–E) Quantification of dendritic branch dynamics for the RGC in (A). (B) Motility rates of terminal branches (n = 109). Branch length at each successive time point (i.e., every 5 min) was measured from branch node to branch tip. (C) Numbers of branches eliminated or added per time interval. (D) Net change in total terminal branch length per time interval. (E) Analysis of branch tip motility. Plots indicate total number of branch tips remaining within 1 µm of the branch tip position in the previous time point. The vast majority of branch tips moved outside of this volume within 5 min.

(F) Plots of terminal branch lifetimes for RGCs analyzed at two ages (n = 3 cells per age). Lifetime measurements were limited to branches present at the initial time point (n = 59). Note that a larger fraction of branches persisted at the older age.

(G) Time-lapse series of RGC with a substantial dendritic arbor prior to lamination in the IPL. Higher magnification of the boxed area shows a new branch forming and then retracting (arrow).

(H) Time-lapse series of RGC with a stratified arbor (Movie S2). The dendritic terminals of stratified cells were relatively more stable compared to RGCs that had yet to stratify.

Error bars in (B) and (F) show standard deviation. dpf, days postfertilization; E, extensions; R, retractions.

innervated deeper parts of the IPL, multiple dendritic strata were resolved (Figures 2A and 2B; Movie S3). By 6 dpf, four GFP-positive strata could be distinguished. Fluorescence intensity plots show that new dendritic strata were added sequentially over time, progressing in a vitreal to scleral order, from the GCL toward the INL (Figure 2C). These strata are positioned at 10%, 40%, 70%, and 90% depth of the IPL (with 0% referring to the GCL/IPL border and 100% to the IPL/INL border; Figure 2D) and were named S^{10}, S^{40}, S^{70}, and S^{90}, accordingly. These data show that RGC dendritic lamination initially proceeds in an "inside-out" temporal order (the inner IPL prior to the outer IPL).

In the second week of development, a fifth stratum, S^{55}, appeared at 55% of IPL depth, apparently emerging in-between S^{40} and S^{70} (Figures 2A–2C). Since this would represent a new pattern of lamination, we tested whether S^{55} arises by intercalation of new dendritic branches or was simply a result of a new outer stratum displacing the relative position of previously resolved strata. For this experiment, we imaged RGC dendritic development in the background of the *Pax6-DF4:MCFP^{Q02}* (*Q02*) transgenic line. The *Q02* line expresses CFP in a subset of amacrine cells whose neuritic arbors stratify primarily within two distinct strata (Godinho et al., 2005), similar to line *pax6DF4:MGFP^{s220t}* (*220*; Kay et al., 2004). At 4 dpf, fluorescence intensity plots show that RGC strata in S^{40} and S^{70} colocalized with the amacrine strata labeled in line *Q02* (Figure 3A). By 6 dpf, a new fluorescence intensity peak of GFP expression appeared between the CFP-labeled amacrine strata at S^{40} and S^{70} (Figure 3, arrowhead), confirming

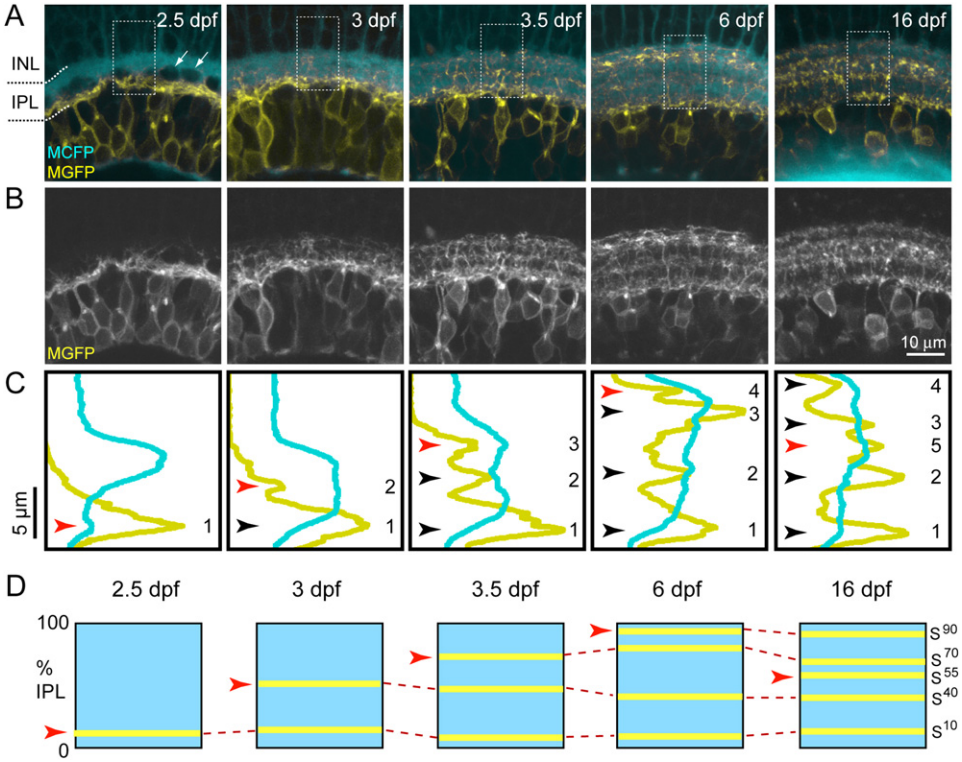

Figure 2. RGC Dendritic Strata Emerge Sequentially in *Brn3c:MGFP* Transgenic Fish

(A) Time-lapse images of a region of retina in a *Brn3c:MGFP/Q01* double-transgenic animal. RGCs express MGFP while the majority of all other retinal cells express MCFP. Each image is an orthogonally oriented 3D projection of a 3 μm thick confocal stack. Arrows indicate displaced amacrine cells (dark profiles) embedded within the IPL at early stages. IPL inner and outer boundaries are marked by dashed lines.

(B) Grayscale images of the MGFP-positive RGCs in (A).

(C) Averaged fluorescence intensities within the boxed regions shown. Arrows indicate peaks in MGFP fluorescence, i.e., strata; red arrows indicate emergence of new strata. Numbers indicate presumed temporal sequence in the appearance of each peak. Five strata are apparent by 16 dpf; stratum 5 appeared to form in-between strata 2 and 3.

(D) Location of each dendritic stratum expressed as a percentage of IPL thickness (e.g., S^{10}; stratum at 10th percentile).

that the fifth stratum, S^{55}, is formed by a process of intercalation of new dendritic branches and likely receives amacrine inputs distinct from those labeled in *Q02*.

RGCs Exhibit Highly Diverse Patterns of Dendritic Targeting

We next explored to what extent individual RGCs followed the global order of IPL stratification observed above. In an extreme case, the sequential lamination could reflect the staggered ingrowth of separate populations of monostratified RGCs, each targeting a distinct stratum. This possibility seemed unlikely, since a substantial fraction of RGCs are multistratified in adult zebrafish (Mangrum et al., 2002). Alternatively, individual RGCs that are bistratified or multistratified may form each of their strata sequentially.

In order to directly observe individual stratification growth patterns, we performed long-term, time-lapse imaging of single, fluorescently labeled RGCs in the background of the *Q01* line. Isolated RGCs expressing MYFP (following DNA injection at the one-cell stage) were found to project dendritic arbors to the same strata as those in the *Brn3c:MGFP* transgenic line (Figure S3).

Our experiments revealed that zebrafish RGCs adopt a multitude of dendritic growth patterns to generate stratified arbors (Figure 4). Strikingly, most of the RGCs we imaged (n = 74 of 83) showed lamina-restricted dendritic arborizations at early stages of IPL innervation. Among these cells, we observed both addition and elimination of strata during the course of development. In a minority of cases, RGCs projected diffusely throughout the depth of the IPL (Figure 4A; n = 9 of 83 cells imaged over time). Invariably, these cells later formed dendritic arbors that ramified in multiple strata and appeared asymmetric in their lateral extension. In contrast to reports in mammals, none of the monostratified zebrafish RGCs we imaged over time (n = 24) initially elaborated dendrites diffusely throughout the entire depth of the IPL. Figure 4B shows an example of a RGC that initially ramified within the inner half of the IPL and later became monostratified within the middle of the IPL. For 21 of 24 monostratified cells imaged, initial dendritic elaboration biases toward the ON or OFF sublamina were predictive of their final lamination pattern. Three of the monostratified cells imaged abandoned an initial lamina in order to target a different stratum later on (Figure 4C).

Most bi- and multistratified RGCs also did not go through a developmental stage in which their arbor was diffusely spread over the IPL depth. Typically (in 41 of 59 cases imaged), these cells formed their dendritic arbors sequentially, first in S^{10}, followed by one

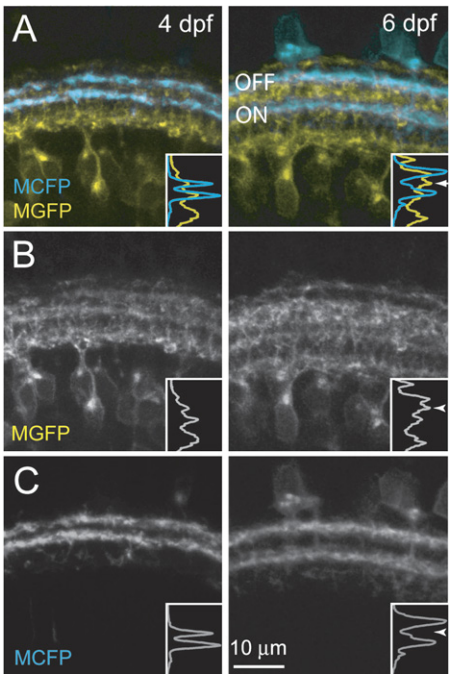

Figure 3. Late RGC Dendritic Stratum Intercalates between Existing Strata

(A) Simultaneous imaging of amacrine cells (MCFP) and RGCs (MGFP) at different ages in *Brn3c:MGFP/Q02* double-transgenic animals. Each image is an orthogonally oriented 3D projection of a 3 μm thick confocal stack. (B and C) Grayscale images providing better detail of the RGC dendrites (B) and amacrine cell neurites (C) shown in (A). At the bottom right corner of each image are the averaged fluorescence intensities within a rectangular region, as in Figure 2. By day 6, the RGC-derived S^{55} stratum appeared in-between the S^{40} and S^{70} strata (arrow in [A]–[C]).

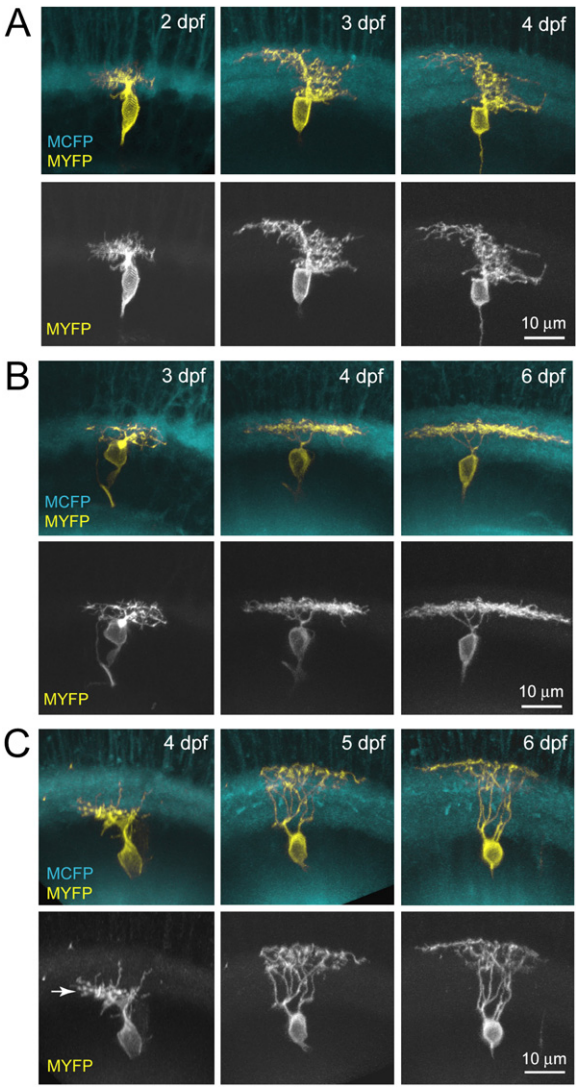

Figure 4. Dendritic Stratification Patterns Resolve from Different Initial Morphologies

Time-lapse imaging of isolated RGCs (MYFP) in the *Q01* background (MCFP). Shown are orthogonally oriented image stacks of the entire arbor. (A) RGC whose dendrites initially elaborated diffusely throughout the depth of the IPL. Later, the cell developed an asymmetrically oriented, multistratified dendritic tree. (B) RGC showing biased elaboration within the inner half of the IPL that later became monostratified, occupying a single stratum in the middle of the IPL. (C) The inner arbor (arrow) of this RGC was lost as the cell went on to develop a monostratified arbor in the OFF sublamina.

or more additional arbors in the outer IPL. Figure 5A shows a representative example of a bistratified RGC in which the inner arbor developed before the outer arbor. In two cases, we also observed the addition of inner dendritic strata after outer strata had formed, perhaps akin to the formation of S^{55} (Figure 5B). However, although the behavior of individual RGCs roughly mirrored the process of inside-out lamination seen for the *Brn3c:MGFP* population, we could not detect a stereotyped sequence in which strata became occupied. Rather, a total of 15 different final stratification patterns were observed. Since some of these patterns were only observed in one out of 83 RGCs imaged, it is likely that our survey was not exhaustive and that additional imaging sessions would discover other growth patterns. Figure 5C provides a summary diagram for those RGCs that were observed to undergo sequential lamination. Finally, we also noted that a single dendritic branch can give rise to terminal dendrites that ramify in both ON and OFF subregions (Figures 6A and 6B, arrows, see also Figure 5A). These dendritic elaborations appear to play a role in expanding field size, as they are evident even after RGC dendrites are stratified.

RGC Dendrites Target Previously Laminated Amacrine Plexuses

Recent imaging studies, using the *Pax6:MGFP^{s220t}* transgenic line, indicated that amacrine cells are capable of forming stratified arborizations in retinas in which RGCs are missing (Kay et al., 2004). In addition, neurite outgrowth between apposing populations of amacrine cells occur around the same time that RGCs begin to extend dendrites (Godinho et al., 2005, see also Figure S2). Moreover, amacrine cell neurites begin to form laminated plexuses almost immediately after becoming directed toward the nascent IPL (Godinho et al., 2005). It is therefore conceivable that amacrine neurites may prepattern the IPL and provide positional cues that help guide RGC dendrites to their correct sublamina. We designed a double-labeling experiment to test whether amacrine stratification preceded that of RGC

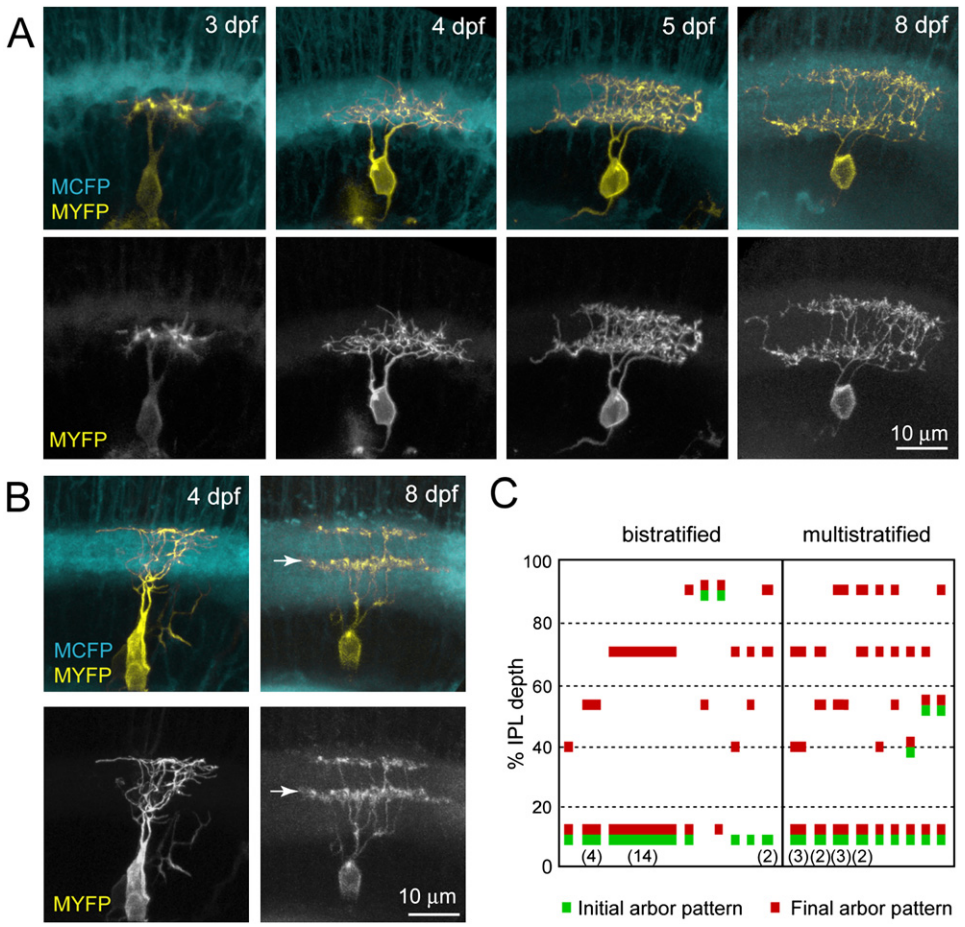

Figure 5. Individual Multistratified RGCs Add Dendritic Strata Sequentially

Time-lapse imaging of isolated RGCs (MYFP) in the *Q01* background (MCFP). Shown are orthogonally oriented image stacks of the entire arbor. (A) Sequential addition of dendritic strata, from inner (ON, S^{10}) to outer (OFF, S^{70}) sublaminae, is evident in this bistratified RGC. (B) Addition of an inner stratum (S^{55}, arrow) to this bistratified cell. (C) Summary of sequential stratification patterns observed for a total of 41 RGCs imaged at at least two ages. Green bars indicate stratification pattern observed at initial time point; red bars at final time point. Numbers in parentheses below bars indicate total number of cells observed with this pattern of strata addition. All others are n = 1.

dendrites. We used the *brn3c* promoter to drive expression of a MYFP reporter in individual RGCs within the *Q02* background. This allowed us to visualize the relative timing of RGC dendrite stratification (YFP signal) versus the appearance of amacrine strata (CFP signal). To guard against the possibility that the *brn3c*-expressing subset of RGCs was somehow unrepresentative (for instance, delayed in their dendrite targeting compared to other RGCs), we also employed the *islet3* promoter to drive mosaic labeling of RGCs. The *islet3* promoter is active in all, or nearly all, RGCs (C-B.C. and A.J.P., unpublished data). For fluorophores, we expressed a membrane-targeted red fluorescent protein (MmCherry; Shaner et al., 2004) in RGCs and used the *Pax6:MGFP^{s220t}* (*220*) transgenic line to simultaneously visualize amacrine cells (Kay et al., 2004). The use of two different combinations of fluorescent reporters increases the confidence that our observations were not biased by differences in expression of fluorescent reporters.

Out of 92 RGCs imaged in the *Q02* and *220* transgenic backgrounds, we successfully observed nine cells that ultimately stratified within the same laminae as labeled amacrine processes. We observed that in every case ON and OFF amacrine-derived strata (S^{40} and S^{70}, respectively) were established prior to the lamination of the RGC dendrites within the same strata (Figure 7). The most common dendritic growth pattern observed involved sequentially stratifying RGCs; after establishing an inner stratum at S^{10}, vertical branches subsequently extended toward and stratified within the S^{40} and/or S^{70} strata (Figures 7A and 7B, arrows). Amacrine cells in the immediate vicinity of these RGCs had already established stratified plexuses in both S^{40} and S^{70} at the earliest time point imaged. A second pattern was exhibited by cells that initially ramified more diffusely, in the inner portion of the IPL (between S^{10} and S^{70}). These cells had arbors that eventually costratified with both of the amacrine-derived plexuses (Figures 7C and 7D). Three different final RGC stratification patterns were observed (Figure 7E). In all cases, and using both RGC promoters, amacrine strata were clearly established prior to corresponding RGC strata. Thus, RGC dendrites can innervate and subsequently costratify with previously established laminar plexuses of amacrine cells.

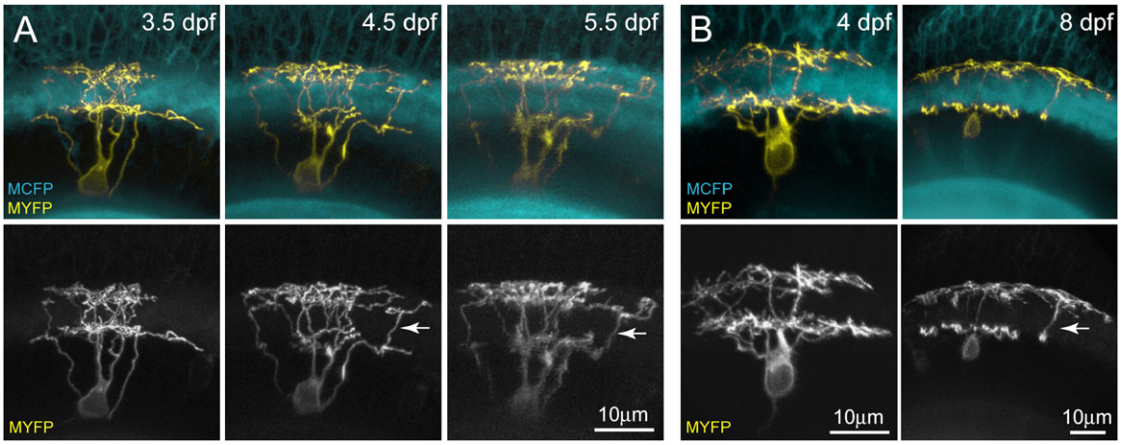

Figure 6. Dendritic Targeting Continues after Lamination Is Established

Time-lapse imaging of isolated RGCs (MYFP) in the *Q01* background (MCFP). (A) Multistratified RGC with a primary dendrite (arrow) that initially stratifies in the ON subregion but later extended and stratified within the OFF subregion. (B) Bistratified RGC with a stratified arbor in the OFF subregion (arrow) extending a branch back into the ON subregion at day 8.

Discussion

Structure and function of CNS neurons are well correlated. However, it is poorly understood how the development of individual neuronal morphologies is coordinated with the formation of the neural circuits in which they participate. To our knowledge, this study is the first example of simultaneous time-lapse imaging, spanning immature to functionally mature stages, of pre- and postsynaptic vertebrate CNS neurons in vivo. The orderly, laminated arrangement of retinal circuitry, particularly within the IPL, provides an excellent model system for investigating the developmental relationship between morphological changes and circuit assembly. We discovered that RGCs exhibit diverse dendritic growth patterns and laminar targeting in order to establish appropriate contact with their afferents (summarized in Figure 8). Our results also implicate amacrine cells as a potential source of lamination cues and provide new insights into how visual circuits are organized during development.

Dendritic Growth Patterns of RGCs: Implications for Visual Circuit Development

By performing long-term, in vivo time-lapse imaging in the zebrafish retina, we uncovered several novel dendritic growth patterns of RGCs. In mammals, static image analyses led to the common view that RGCs initially elaborate dendrites diffusely throughout the depth of the IPL (Maslim et al., 1986; Dann et al., 1988; Ramoa et al., 1988; Bodnarenko et al., 1995, 1999), making indiscriminate connections early on (Wang et al., 2001; Tian and Copenhagen, 2003). A large number of mature mammalian RGCs are monostratified, in either ON or OFF sublaminae, suggesting that branch elimination is the primary mechanism by which dendritic stratification of RGCs is ultimately achieved (reviewed by Sernagor et al., 2001; Chalupa and Gunhan, 2004; Xu and Tian, 2004; Figure 8). Thus, by extrapolation to other vertebrates, it has been assumed that RGC dendritic stratification occurs generally via a loss of dendrites from inappropriate synaptic locations. Indeed, dendritic pruning appears to be a key mechanism by which many types of CNS neurons attain their final arbor shape and connectivity patterns (Wong and Ghosh, 2002).

Although we did observe significant dendritic pruning in some zebrafish RGCs (e.g., Figure 4C), we found that in contrast to mammals the dendrites of the majority of zebrafish RGCs grew in a biased manner toward their laminar target zone(s) within the IPL. Monostratified zebrafish RGCs showed early patterns of dendritic outgrowth that were predictive of their final lamination patterns. Also, dendritic arbors of the majority of bistratified and multistratified zebrafish RGCs were generated sequentially over time, rather than sculpted from a diffuse arbor by branch elimination. Because we had to limit the frequency of image acquisition in order to avoid phototoxic effects, it is conceivable that some RGCs exhibited a transient phase of diffuse dendritic elaboration not apparent within our recording periods. However, we also observed that net growth and significant changes in RGC arborization patterns occur on a relatively protracted time scale, making it unlikely that major structural changes were missed, especially given the large number of cells (>300) imaged by time-lapse methods. Thus, we conclude that for many zebrafish RGCs, dendritic arbors do not undergo a period of significant pruning, as might be expected from previous work on mammals (Sernagor et al., 2001; Chalupa and Gunhan, 2004; Xu and Tian, 2004).

The sequential addition of dendritic strata of individual and populations of RGCs also has implications for how visual circuits are assembled. This pattern of dendritic growth suggests that distinct visual processing circuits involving RGCs may not become functional at the same rate. We found that dendritic stratification in bistratified and multistratified RGCs proceeded largely from vitreal (inner, ON) to scleral (outer, OFF) sublaminae in the IPL. This inside-out sequence was not a strict rule, however, because new dendritic strata could also appear in-between existing strata (e.g., S^{55}, the fifth stratum to form). Interestingly, RGC input to the tectum becomes active by 66 hpf, and most tectal neurons display mature response properties as early as 78 hpf (Niell

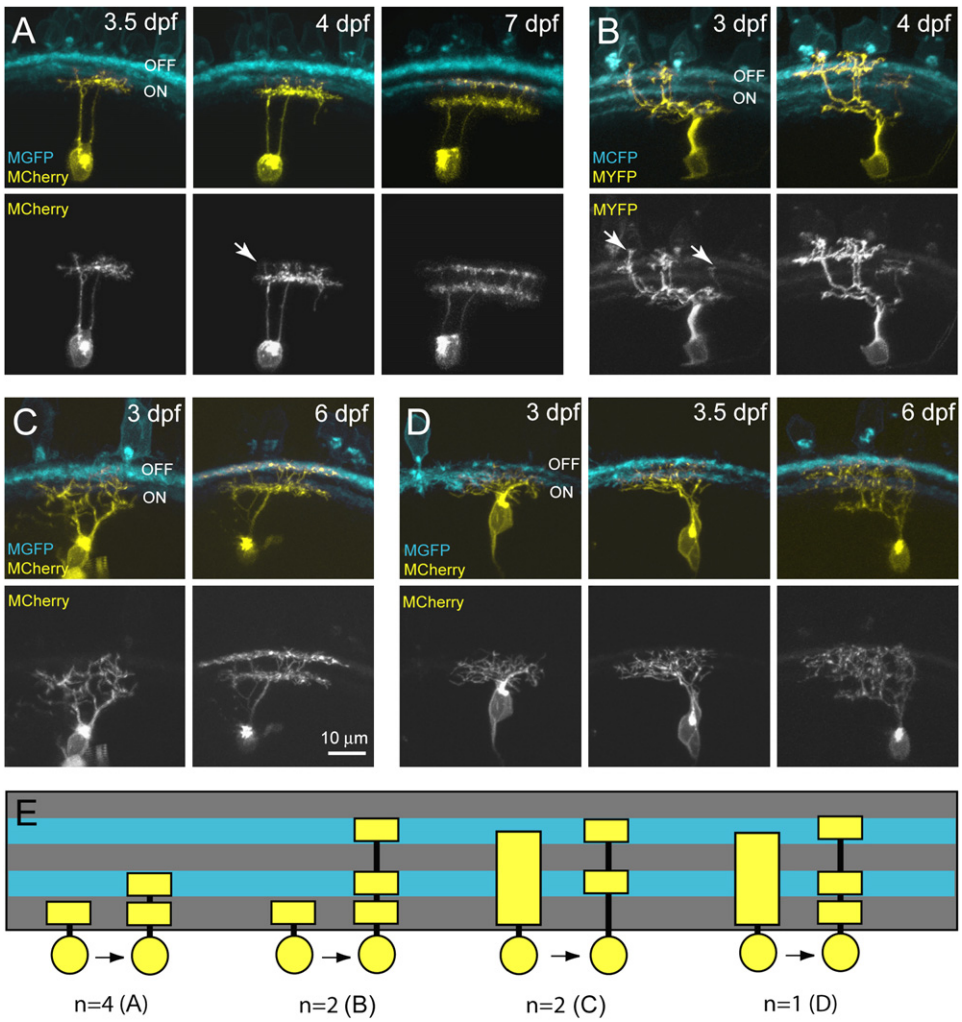

Figure 7. RGC Dendrites Target Established Presynaptic Amacrine Strata

Simultaneous time-lapse imaging of costratifying RGCs and amacrine cells. Injection of either an *islet3:MCherry* plasmid construct into the 220 background (A, C, and D) or *brn3c:MYFP* plasmid construct into the *Q02* background (B) was used to express reporter proteins in individual RGCs. (A and B) Vertical extensions of stratified RGC arbors (arrows) appear to target previously established amacrine-derived strata. New RGC strata subsequently extended from these processes in both the ON (A) and OFF (B) subregions. (C and D) Cells with dendritic distributions initially biased toward the inner IPL subsequently restricted their dendrites to at least one or more labeled amacrine-derived strata. (E) Schematic summarizing dendritic growth patterns observed for RGCs that targeted labeled amacrine-derived strata. Figures (A)–(D) represent examples of each of the four types of RGC growth patterns observed.

and Smith, 2005). This study, together with ours, suggests that RGCs are capable of performing advanced processing functions several days before structural development is complete in both their dendritic and axonal terminals (Niell et al., 2004).

Dendritic Targeting as a Mechanism for Achieving Circuit Specificity

By imaging individual RGCs in vivo across their period of dendritic development, we discovered that dendrites target their future synaptic laminae where axons have already formed their terminal plexuses. Our current findings contrast with previous work showing that precision in circuit assembly is determined by axons specifically targeting their future synaptic laminae during development (Eide and Glover, 1997; Ozaki and Snider, 1997; Clandinin and Zipursky, 2000; Miller et al., 2001; Ting et al., 2005; reviewed by Sanes and Yamagata, 1999). Our current observations, together with previous work, support the concept that dendritic targeting, in addition to axonal targeting, is an important mechanism in setting up CNS circuits (Morest, 1969; Saito et al., 1992; Jontes and Smith, 2000). For example, in the *Drosophila* olfactory system, second-order projection neurons (PNs) elaborate dendrites in a highly stereotypical manner, creating a template of the mature glomerular map, prior to the arrival of the olfactory sensory axons (Jefferis et al., 2004). Homotypic attraction and heterotypic repulsion between dendrites of specific subtypes of PN neurons are believed to be essential for this early patterning. Sensory axons then target PN dendritic arbors that are already localized to the correct parts of the antennal lobe. However, in contrast to *Drosophila* PN neurons, RGC dendrites grow toward previously established axonal terminals of presynaptic amacrine cells. Thus, whereas dendritic targeting by *Drosophila*

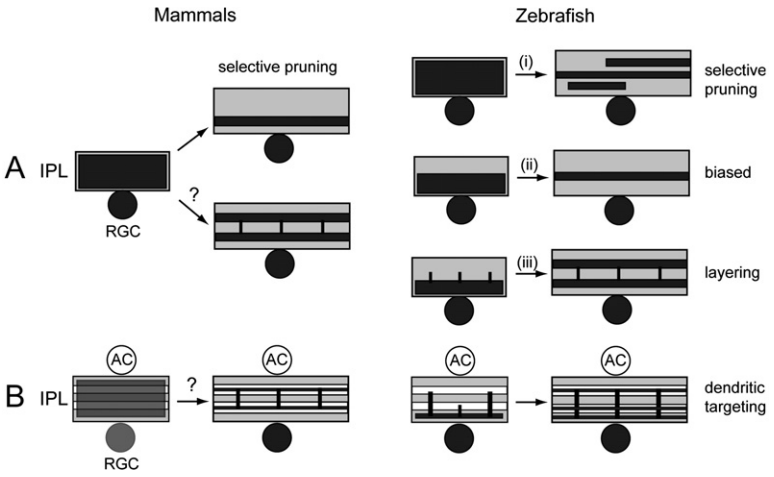

Figure 8. Summary of Dendritic Lamination Strategies of RGCs

Comparison of the lamination strategies in mammals and zebrafish. (A) In mammals, immature RGC dendrites are thought to occupy the entire depth of the IPL; dendrites occupying inappropriate regions are then selectively eliminated ("pruned") to form discrete strata. For technical reasons, mammalian studies have been limited to static imaging and have thus far focused on monostratified RGC subtypes; how bistratified and multistratified RGCs achieve their adult lamination patterns in mammals is not clear (denoted by question mark). Using in vivo time-lapse imaging in zebrafish we followed individual RGCs from immature to mature states and thereby correlate early arborization morphologies with final stratification patterns. Our analysis included observations of the dendritic behavior of mono-, bi-, and multistratified RGCs. We found several growth patterns by which the dendrites of zebrafish RGCs attain laminated arbors. (i) A particular multistratified RGC subtype was observed to behave more like mammalian RGCs; initially the dendritic arbor occupied the entire depth of the IPL, and subsequently an asymmetric multistratified arbor emerged. (ii) Most monostratified zebrafish RGCs showed a dendritic elaboration that is biased to the subregion of the IPL within which they later stratify. None of the monostratified RGCs we observed ramified throughout the IPL at early stages. (iii) The majority of bi- and multistratified RGCs demonstrated sequential layering of dendritic strata; strata can be added from the inner to the outer IPL, vice versa, or even in-between existing strata. (B) In mammals, cholinergic amacrines appear to form laminated plexuses prior to the stratification of bistratified RGCs (Stacy and Wong, 2003). However, morphological identification of immature bistratified RGCs is problematic, making it difficult to ascertain the dendritic growth pattern of this subtype of RGC. In zebrafish, time-lapse analyses demonstrate that amacrine cells form laminated plexuses prior to the stratification of RGC dendrites within these same laminae. RGC dendrites thus appear to target and subsequently costratify with prepatterned afferent plexuses.

PNs is achieved by interactions among dendrites, zebrafish RGCs may utilize a laminar scaffold provided by axonal terminals.

Can amacrine cells influence dendritic targeting of the IPL by RGCs? Our observations in this and earlier studies (Kay et al., 2004; Godinho et al., 2005) suggest that dendritic development by RGCs can be broken down into distinct phases, each possibly involving signaling from amacrine cells: (1) directed outgrowth of RGC dendrites toward an early amacrine plexus, (2) targeting by RGC dendrites to the appropriate IPL laminar depth, and (3) stabilization of exploratory dendritic branches opposite presynaptic amacrine cell axons, potentially by a synaptotropic mechanism. In the following, we discuss how amacrine cells could affect RGC dendritic arborization patterns and, thereby, shape retinal circuit formation.

RGCs initially extend dendrites from their location in the inner retina in the direction of the amacrine cells. Early on, a thin plexus forms between an inner and outer population of amacrine cells (Figure S2; Godinho et al., 2005). At this stage, RGC dendrites accumulate beneath the innermost layer of the amacrine cells (displaced amacrine cells) and later bypass them to join up with the amacrine-derived plexus. Thus, the displaced amacrine cells are initially embedded within the nascent IPL, in a location where they could influence early dendritic elaborations of RGCs (Figures 2A and 5A; Figure S2). We have no direct evidence that RGC dendritic growth is influenced by the displaced amacrine cells, but previous studies in mouse have implicated amacrine cells in providing a contact-dependent signal that stimulates RGC dendritic growth (Goldberg et al., 2002).

The amacrine plexus becomes laminated at an early stage, shortly following the establishment of polarized amacrine neurite outgrowths (Godinho et al., 2005) and well before RGC dendrite stratification is observed within the same regions (this study). This is in agreement with a study in mice that showed that processes of the cholinergic amacrine subtype stratify before those of RGCs (Stacy and Wong, 2003). Here we observed directly, in double-labeling experiments, that RGC dendrites appear to target prelaminated amacrine neurites soon after entering the IPL. In *lakritz* mutants, which lack all RGCs due to mutation of the proneural transcription factor Atoh7 (Ath5), amacrine neurites are initially disorganized, but form sublaminae after a short delay (Kay et al., 2004). This experiment ruled out an essential role for RGCs in IPL stratification for amacrine cells. However, the sequence of lamination observed here (amacrines before RGCs) argues that amacrine cells could provide a laminar scaffold for their RGC partners. This model makes the prediction that RGCs should be unable to form stratified dendrites in the absence of amacrine cells. While the crucial experiment has not yet been carried out, ablation of cholinergic amacrine cells in ferrets did not disrupt IPL sublamination (Reese et al., 2001). However, in this study, amacrine cells were killed postnatally, after RGC dendrites may have attained a significant degree of stratification and/or the IPL may already have been patterned. Moreover the cholinergic cells represent only a small fraction of all amacrine cells. Future experiments in which amacrine cells are ablated or fail to differentiate, in combination with labeling of RGCs that normally contact the ablated subtype, are needed to directly address the potential role of amacrine cells in dendritic stratification.

Although our dynamic imaging of pre- and postsynaptic interactions suggests that RGC dendrites follow amacrine axons, we cannot exclude the possibility that both amacrine cells and RGCs are responsive to the same molecular factors arrayed within the extracellular

matrix of the IPL. For example, bipolar cell axons (Schmitt and Dowling, 1999) and Müller glial cell processes (Peterson et al., 2001) are present in the developing zebrafish IPL prior to when RGC dendritic stratification is completed. Thus, it will also be important to ascertain the developmental role of all retinal cell types that contribute processes to the forming IPL in zebrafish and to identify molecular stratification cues in addition to the *sidekicks* (Yamagata et al., 2002).

What is the mechanism underlying dendrite targeting? Are the tips of dendrites guided to their sublamina by chemotropic guidance cues, similar to axonal growth cones? Or, is target recognition achieved by a mechanism of unguided exploration and selective stabilization? Our rapid time-lapse studies indicate that the second scenario may hold true. We observed that RGC dendrites actively probed their microenvironment as they invaded the IPL, rapidly extending and retracting branches. We further saw that RGC dendrites switched to a more stable growth mode, following stratification. This suggests a synaptotropic mechanism by which synaptogenesis shapes dendritic arbors as they are forming (Vaughn et al., 1988). Other in vivo imaging studies of dendritic growth have demonstrated the same type of dynamism (Rajan and Cline, 1998; Wu et al., 1999; Lendvai et al., 2000; Niell et al., 2004). In the retinotectal projection, stabilization of dendrites is highly correlated with the presence of nascent synaptic inputs (Niell et al., 2004). Thus, we propose that RGC dendrites recognize their correct stratum upon contact with amacrine axons or some other presynaptic partner. Their laminar choice may be mediated by molecular cues expressed on the presynaptic cell surface and reinforced by the onset of synaptic transmission (e. g., Bansal et al., 2000; Lohmann et al., 2002; Stacy et al., 2005).

In summary, sequential addition of dendritic strata is a novel growth pattern that suggests that connections between RGCs and functionally distinct subsets of presynaptic neurons may be formed in a specific temporal order, with the exact order varying between RGC subtypes. Furthermore, time-lapse sequences suggest that RGC dendrites directly target regions where amacrine cells have already established stable, laminated afferent patterns. This finding contrasts with the commonly regarded notion that afferents play the active role in seeking out synaptic partnerships and supports the emerging view that dendrites can also exhibit directed outgrowth during circuit assembly.

Experimental Procedures

Zebrafish Lines Utilized

All zebrafish lines were maintained at 28.5°C and bred naturally according to a 14 hr ON/10 hr OFF light cycle. Transgenic zebrafish lines utilized here include (1) *Tg(Brn3c:gap43-GFP)^{s356t}*, or *Brn3c:MGFP*, which expresses membrane-tagged GFP (MGFP) in approximately 50% of RGCs (Xiao et al., 2005); (2) *Tg(Pax6-DF4:gap43-GFP)^{s220t}*, or *220*, which expresses MGFP in a large subpopulation of amacrine cells that form stratified arborizations in discrete ON and OFF sublaminae (Kay et al., 2004); (3) *Tg(Pax6-DF4:gap43-CFP)^{q01}*, or *Q01*, which expresses membrane-tagged CFP (MCFP) throughout the retina (Godinho et al., 2005); (4) *Tg(Pax6-DF4:gap43-CFP)^{q02}*, or *Q02*, which expresses MCFP in a small subset of amacrine cells that form stratified arborizations in discrete ON and OFF sublaminae (Godinho et al., 2005); and (5) *Tg(ptf1a:GFP)*, or *ptf1a*, which expresses GFP in all amacrine interneurons (Lin et al., 2004; Godinho et al., 2005). These lines are referred to throughout the text as *Brn3c:MGFP*, *220*, *Q01*, *Q02*, and *ptf1a*, respectively. For all imaging experiments, 1-phenyl-2-thiourea (PTU) was used to inhibit melanin formation in embryonic and larval fish (200 μM final concentration, added to embryo medium at 16 hpf). In addition, the majority of these experiments (except those utilizing *ptf1a:GFP* embryos) were performed in the background of a pigmentation mutant, *roy* (*roy orbison*; Ren et al., 2002), in which iridophores are reduced. By reducing the amount of reflective pigment, *roy* mutants facilitate high-resolution imaging of the retina at later ages (i.e., beyond the third day of development). The retina of *roy* mutants, and in particular the IPL, has been shown to be morphologically normal, and these mutants perform indistinguishably from wild-type in several visual performance tasks (Ren et al., 2002).

Transient Expression of Fluorescent Reporter in Individual RGCs

DNA injected into fertilized eggs resulted in expression of fluorescent protein in isolated RGCs. Typically, anywhere from 1 to 20 RGCs were labeled in individual eyes that were selected for imaging. All injections were performed as previously described (Lohmann et al., 2005). In order to increase reporter expression levels, the Gal4-VP16/14XUAS system was utilized (Köster and Fraser, 2001). Specifically, either (1) a *brn3c:Gal4-VP16* driver and 14X*UAS:gap43-YFP* reporter or (2) an *islet3:gap43-mCherry* reporter construct were injected into one cell stage eggs from *Q01;roy*, *Q02;roy*, *220;roy*, or *ptf1a:GFP* matings, according to complementary color schemes (e.g., cyan/yellow or green/red). The *brn3c:Gal4-VP16* driver construct was derived from the pTR56 (Xiao et al., 2005) and pCSGal4-VP16 plasmids (Köster and Fraser, 2001). The 14X*UAS:gap43-YFP* reporter construct was derived from 14XUAS (Köster and Fraser, 2001) and *pax6-DF4:MYFP* (Godinho et al., 2005). The *islet3:gap43-mCherry* reporter construct uses 17.6 kb of upstream genomic sequence from the *islet3* (*isl3*) gene (A.J.P. and C.-B.C., unpublished data) to drive membrane-targeted monomeric Cherry (MmCherry; Shaner et al., 2004). Complete cloning details are available upon request.

Embryos were screened for expression of both reporters (stable and/or transient expression derived) in the retina at 36–44 hpf. Double-positive embryos were screened again using confocal microscopy to identify those that had expression of the reporter (MYFP or MmCherry) in individual or isolated subsets of RGCs. Isolated RGCs were imaged from the time of initial dendritic outgrowth until stratified arborizations were evident. The timing of this process was position dependent (following the general wave of retinal differentiation which sweeps from the ventral/nasal to the dorsal/temporal region) within individual fish. Thus, strict temporal correlations regarding differentiation stages between individual cells across fish were not possible. For this reason, we chose to delineate time in terms of days postfertilization rather than hours postfertilization. Also, some injected embryos were initially maintained at room temperature (25°C) from 12 to 24 hpf in order to delay differentiation and thereby maximize the number of RGCs that could be observed at immature time points. Subsequently, all embryos/larvae were maintained at 28.5°C. For all embryos that were temporarily maintained at 25°C, developmental timing estimates were subsequently scaled accordingly.

Immunocytochemistry

Cryosections were incubated overnight in mouse zn5 antibody (1:500, Zebrafish International Resource Center) diluted in 0.1 M PBS and containing 0.5% Triton X-100. Alexa Fluor 633 conjugated Phalloidin (1:50; Molecular Probes) was included in the primary antibody incubation to reveal the general architecture of the retina. The sections were then washed several times in 0.1 M PBS and incubated in a secondary antibody; Alexa Fluor 568 goat anti-mouse (Molecular Probes) diluted 1:1000 in 0.1 M PBS, for 1 hr. After several washes in 0.1 M PBS, sections were coverslipped in Vectashield (Vector Laboratories).

In Vivo Confocal Microscopy

All live imaging was performed as previously described (Kay et al., 2004; Godinho et al., 2005; Lohmann et al., 2005) with the exception that a "catch and release" protocol was developed for monitoring

individual RGCs over multiple days. Briefly, fish imaged for prolonged periods were individually embedded in agarose drops on glass slides prior to each imaging session. Fish were oriented such that retinas were imaged from the lateral view. After the agarose solidified, slides were flooded with 0.3× Danieau's solution containing PTU and tricaine and maintained at 28.5°C. Following each imaging session, individual agarose drops were gently pried apart with forceps until the embedded fish was released into the overlying buffer solution. Embryos/larvae were then rinsed in 0.3× Danieau's solution and placed individually in labeled wells of a multiwell tray. Between imaging sessions, all embryos/larvae were maintained in 0.3× Danieau's solution containing PTU (without tricaine) at 28.5°C. For subsequent imaging sessions, fish were embedded in agarose as above, and previously imaged cells were identified according to retinal position and morphology.

All images were acquired on an Olympus FV500 laser scanning confocal microscope, using a 60× (NA 1.1, Olympus) long working distance water objective. Per time point, a series of optical sections in the z dimension was acquired spanning the area of interest (e.g., for individual RGCs, z dimension "stacks" include the entire arborization). To visualize GFP and CFP together it was necessary to image each channel sequentially due to overlap between the excitation source for GFP (488 nm laser line) and the emission spectra captured for CFP. For all other combinations, reporters were imaged simultaneously. For long-term experiments, individual RGCs were imaged at daily intervals, as attempts to image more frequently over long periods showed evidence of phototoxicity. For analyses of terminal branch dynamics, RGCs were imaged every 5 min for 30 min total.

Image Processing and Analysis

For consistency, all amacrine cells and RGCs were pseudocolored cyan and yellow, respectively, regardless of the emission profile of the reporter fluorophore utilized. 3D image rendering and analyses of dendrite dynamics were performed using Amira (TGS Template Graphics software). Prior to 3D reconstruction, all image stacks were processed using Metamorph (Universal Imaging; median filtration) to reduce background noise. Some images were further processed to enhance signal-to-noise ratios or optimize colors using Adobe Illustrator and/or Photoshop. All images shown are orthogonally oriented 3D projections—orthogonal position determined by adjusting rotational aspects of 3D images rendered in Amira (voltex function). During imaging of populations of amacrine and RGCs, a series of optical sections in the z dimension bracketing the orthogonal plane was collected (36 sections at 0.28 μm steps for a total of 10 μm). For the sake of clarity, however, images of populations of amacrine and RGCs were limited to 3 μm in the z dimension. Images of individual RGCs, however, include the entire dendritic arbor. Fluorescence intensity plots were performed using the MetaMorph linescan function (average intensity) to analyze stratification patterns in the images presented ("line" width was typically 200 pixels, and relative intensities were adjusted such that the strongest signal in each plot peaked at approximately the 90th percentile).

To measure changes in dendrite length over time, the distance between tip and branch point (or point of origin on cell) of terminal branches was measured using the line probe function of Amira. Measurements of net branch addition/elimination, net change in dendrite length, and average/maximal extension and retraction rates were derived by monitoring all terminal branches of the cell over time (i.e., those present at any time during the 30 min recording period). Measurements of termini stability were obtained by mapping each dendrite tip in 3D space (Amira, label field function) and determining whether the tip was present or absent from a sphere with radius of 1 μm, centered at the previous position, for each successive time point. Measurements of branch persistence were obtained by determining whether branches evident at the beginning of the recording were present at each subsequent time point until the end of the 30 min recording period.

In one case, we had to digitally highlight a particular RGC (Figure 7A) in order to display its dendritic arbor separately from nearby, labeled cells in the same field of view. Dendrites of this RGC were traced using the Amira label field function. Individual branches were labeled plane by plane in the z dimension in order to ensure accuracy. Supplementary time-lapse movies and image rotations were created using Amira voltex, animate, time, and moviemaker functions; movies were subsequently compressed using Quicktime Pro.

Supplemental Data

The Supplemental Data for this article can be found online at http://www.neuron.org/cgi/content/full/52/4/609/DC1/.

Acknowledgments

This work was supported by NIH grants to R.O.L.W. (EY14358), C-B.C. (EY12873), and H.B. (EY13855 and EY12406); an NRSA predoctoral fellowship (NIH/NINDS) to A.J.P.; and an NRSA postdoctoral fellowship (NIH/NEI) to J.S.M. H.B. was a David and Lucile Packard Fellow. We thank Ben Mangum for help with *isl3* constructs and Josh Morgan and Meera Saxena for helpful comments on the manuscript. The experimental procedures used in this study were approved by the Washington University Institutional Animal Care and Use Committee and complied with all relevant regulations regarding the use of vertebrate organisms for research purposes.

Received: February 1, 2006
Revised: August 25, 2006
Accepted: October 5, 2006
Published: November 21, 2006

References

Bansal, A., Singer, J.H., Hwang, B.J., Xu, W., Beaudet, A., and Feller, M.B. (2000). Mice lacking specific nicotinic acetylcholine receptor subunits exhibit dramatically altered spontaneous activity patterns and reveal a limited role for retinal waves in forming ON and OFF circuits in the inner retina. J. Neurosci. *20*, 7672–7681.

Bodnarenko, S.R., Jeyarasasingam, G., and Chalupa, L.M. (1995). Development and regulation of dendritic stratification in retinal ganglion cells by glutamate-mediated afferent activity. J. Neurosci. *15*, 7037–7045.

Bodnarenko, S.R., Yeung, G., Thomas, L., and McCarthy, M. (1999). The development of retinal ganglion cell dendritic stratification in ferrets. Neuroreport *10*, 2955–2959.

Burrill, J.D., and Easter, S.S., Jr. (1995). The first retinal axons and their microenvironment in zebrafish: cryptic pioneers and the pretract. J. Neurosci. *15*, 2935–2947.

Cajal, S.R. (1972). The Structure of the Retina, S.A. Thorpe and M. Glickstein, translators (Springfield, IL: Charles C Thomas Press).

Chalupa, L.M., and Gunhan, E. (2004). Development of On and Off retinal pathways and retinogeniculate projections. Prog. Retin. Eye Res. *23*, 31–51.

Clandinin, T.R., and Zipursky, S.L. (2000). Afferent growth cone interactions control synaptic specificity in the Drosophila visual system. Neuron *28*, 427–436.

Dann, J.F., Buhl, E.H., and Peichl, L. (1988). Postnatal dendritic maturation of alpha and beta ganglion cells in cat retina. J. Neurosci. *8*, 1485–1499.

Easter, S.S., Jr., and Nicola, G.N. (1996). The development of vision in the zebrafish, Danio rerio. Dev. Biol. *180*, 646–663.

Easter, S.S., Jr., and Nicola, G.N. (1997). The development of eye movements in the zebrafish (*Danio rerio*). Dev. Psychobiol. *31*, 267–276.

Eide, A.L., and Glover, J.C. (1997). Developmental dynamics of functionally specific primary sensory afferent projections in the chicken embryo. Anat. Embryol. (Berl.) *195*, 237–250.

Famiglietti, E.V.J., and Kolb, H. (1976). Structural basis for ON- and OFF-center responses in retinal ganglion cells. Science *194*, 193–195.

Godinho, L., Mumm, J.S., Williams, P.R., Schroeter, E.H., Koerber, A., Park, S.W., Leach, S.D., and Wong, R.O.L. (2005). Targeting of amacrine cell neurites to appropriate synaptic laminae in the developing zebrafish retina. Development *132*, 5069–5079.

Goldberg, J.L., Klassen, M.P., Hua, Y., and Barres, B. (2002). Amacrine-signaled loss of intrinsic axon growth ability by retinal ganglion cells. Science *296*, 1860–1864.

Hu, M., and Easter, S.S. (1999). Retinal neurogenesis: the formation of the initial central patch of postmitotic cells. Dev. Biol. *207*, 309–321.

Jan, Y.-N., and Jan, L.Y. (2003). The control of dendrite development. Neuron *40*, 229–242.

Jefferis, G.S.X.E., Vyas, R.J., Berdnik, D., Ramaekaers, A., Stocker, R.F., Tanaka, N.K., Ito, K., and Luo, L. (2004). Developmental origin of wiring specificity in the olfactory system of *Drosophila*. Development *131*, 117–130.

Jontes, J.D., and Smith, S.J. (2000). Filopodia, spines, and the generation of synaptic diversity. Neuron *27*, 11–14.

Jontes, J.D., Buchanan, J., and Smith, S.J. (2000). Growth cone and dendrite dynamics in zebrafish embryos: early events in synaptogenesis imaged in vivo. Nat. Neurosci. *3*, 231–237.

Katz, L.C., and Crowley, J.C. (2002). Development of cortical circuits: lessons from ocular dominance columns. Nat. Rev. Neurosci. *3*, 34–42.

Kay, J.N., Roeser, T., Mumm, J.S., Godinho, L.N., Mrejeru, A., Wong, R.O.L., and Baier, H. (2004). Transient requirement for ganglion cells during assembly of retinal stnaptic layers. Development *131*, 1332–1341.

Komiyama, T., and Luo, L. (2006). Development of wiring specificity in the olfactory system. Curr. Opin. Neurobiol. *16*, 1–7.

Köster, R.W., and Fraser, S.E. (2001). Tracing transgene expression in living zebrafish embryos. Dev. Biol. *233*, 329–346.

Lendvai, B., Stern, E.A., Chen, B., and Svoboda, K. (2000). Experience-dependent plasticity of dendritic spines in the developing rat barrel cortex *in vivo*. Nature *404*, 876–881.

Lettvin, J.Y., Maturana, H.R., McCulloch, W.S., and Pitts, W.H. (1959). What the frog's eye tells the frog's brain. Proc. Inst. Radio Engr. *47*, 1940–1951.

Lin, J.W., Biankin, A.V., Horb, M.E., Ghosh, B., Prasad, N.B., Yee, N.S., Pack, M.A., and Leach, S.D. (2004). Differential requirement for ptf1a in endocrine and exocrine lineages of developing zebrafish pancreas. Dev. Biol. *274*, 491–503.

Lohmann, C., Myhr, K.L., and Wong, R.O.L. (2002). Transmitter-evoked local calcium release stabilizes developing dendrites. Nature *418*, 177–181.

Lohmann, C., Mumm, J., Morgan, J., Godinho, L., Schroeter, E., Stacy, R., Wong, W.T., Oakley, D.M., and Wong, R.O.L. (2005). Imaging the developing retina. In Imaging in Neuroscience and Development, R. Yuste and A. Konnerth, eds. (Cold Spring Harbor, NY: CSHL Press), pp. 171–184.

Luo, L., and O'Leary, D.M. (2005). Axon retraction and degeneration in development and disease. Annu. Rev. Neurosci. *28*, 127–156.

Mangrum, W.I., Dowling, J.E., and Cohen, E.D. (2002). A morphological classification of ganglion cells in the zebrafish retina. Vis. Neurosci. *19*, 767–779.

Maslim, J., Webster, M., and Stone, J. (1986). Stages in the structural differentiation of retinal ganglion cells. J. Comp. Neurol. *254*, 382–402.

McAllister, A.K. (2000). Cellular and molecular mechanisms of dendritic growth. Cereb. Cortex *10*, 963–973.

Miller, B., Blake, N.M., Erinjeri, J.P., Reistad, C.E., Sexton, T., Admire, P., and Woolsey, T.A. (2001). Postnatal growth of intrinsic connections in mouse barrel cortex. J. Comp. Neurol. *436*, 17–31.

Morest, D.K. (1969). The differentiation of cerebral dendrites: A study of the post-migratory neuroblast in the medial nucleus of the trapezoid body. Z. Anat. Entwicklungsquesch *128*, 271–289.

Mumm, J.S., Godinho, L., Morgan, J.L., Oakley, D.M., Schroeter, E.H., and Wong, R.O.L. (2005). Laminar circuit formation in the vertebrate retina. Prog. Brain Res. *147*, 155–169.

Niell, C.M., and Smith, S.J. (2005). Functional imaging reveals rapid development of visual response properies of zebrafish tectum. Neuron *45*, 941–951.

Niell, C.M., Meyer, M.P., and Smith, S.J. (2004). In vivo imaging of synapse formation on a growing dendritic arbor. Nat. Neurosci. *7*, 254–260.

Ozaki, S., and Snider, W.D. (1997). Initial trajectories of sensory axons toward laminar targets in the developing mouse spinal cord. J. Comp. Neurol. *380*, 215–229.

Peterson, R.E., Fadool, J.M., McClintock, J., and Linser, P.J. (2001). Muller cell differentiation in the zebrafish neural retina: evidence of distinct early and late stages in cell maturation. J. Comp. Neurol. *429*, 530–540.

Rajan, I., and Cline, H.T. (1998). Glutamate receptor activity is required for normal development of tectal cell dendrites in vivo. J. Neurosci. *18*, 7836–7846.

Ramoa, A.S., Campbell, G., and Shatz, C.J. (1988). Dendritic growth and remodeling of cat retinal ganglion cells during fetal and postnatal development. J. Neurosci. *8*, 4239–4261.

Reese, B.E., Raven, M.A., Giannotti, K.A., and Johnson, P.T. (2001). Development of cholinergic amacrine cell stratification in the ferret retina and the effects of early excitotoxic ablation. Vis. Neurosci. *18*, 559–570.

Ren, J.Q., McCarthy, W.R., Zhang, H., Adolph, A.R., and Li, L. (2002). Behavioral visual responses of wild-type and hypopigmented zebrafish. Vision Res. *42*, 293–299.

Roska, B., and Werblin, F. (2001). Vertical interactions across ten parallel, stacked representations in the mammalian retina. Nature *410*, 583–587.

Saito, Y., Murakami, F., Song, W.J., Okawa, K., Shimono, K., and Katsumaru, H. (1992). Developing corticorubral axons of the cat form synapses on filopodial dendritic protrusions. Neurosci. Lett. *147*, 81–84.

Sanes, J.R., and Yamagata, M. (1999). Formation of lamina-specific synaptic connections. Curr. Opin. Neurobiol. *9*, 79–87.

Schmitt, E.A., and Dowling, J.E. (1999). Early retinal development in the zebrafish, Danio rerio: light and electron microscopic analyses. J. Comp. Neurol. *404*, 515–536.

Sernagor, E., Eglen, S.J., and Wong, R.O. (2001). Development of retinal ganglion cell structure and function. Prog. Retin. Eye Res. *20*, 139–174.

Shaner, N.C., Campbell, R.E., Steinbach, P.A., Giepmans, B.N., Palmer, A.E., and Tsien, R.Y. (2004). Improved monomeric red, orange and yellow fluorescent proteins derived from Discosoma sp. red fluorescent protein. Nat. Biotechnol. *22*, 1567–1572.

Stacy, R.C., and Wong, R.O.L. (2003). Developmental relationship between cholinergic amacrine cell processes and ganglion cell dendrites of the mouse retina. J. Comp. Neurol. *456*, 154–166.

Stacy, R., Demas, J., Burgess, R., Sanes, J.R., and Wong, R.O.L. (2005). Disruption and recovery of patterned retinal activity in the absence of acetylcholine synthesis. J. Neurosci. *25*, 9347–9357.

Stuermer, C.A.O. (1988). Retinotopic organization of the developing retinotectal projection in the zebrafish embryo. J. Neurosci. *8*, 4513–4530.

Tian, N., and Copenhagen, D.R. (2003). Visual stimulation is required for refinement of ON and OFF pathways in postnatal retina. Neuron *39*, 85–96.

Ting, C.Y., Yonekura, S., Chung, P., Hsu, S.N., Robertson, H.M., Chiba, A., and Lee, C.H. (2005). Drosophila N-cadherin functions in the first stage of the two-stage layer-selection process of R7 photoreceptor afferents. Development *132*, 953–963.

Vaughn, J.E., Barber, R.P., and Sims, T.J. (1988). Dendritic development and preferential growth into synaptogenic fields: A quantitative study of Golgi-impregnated spinal motor neurons. Synapse *2*, 69–78.

Wang, G.Y., Liets, L.C., and Chalupa, L.M. (2001). Unique functional properties of on and off pathways in the developing mammalian retina. J. Neurosci. *21*, 4310–4317.

Wässle, H. (2004). Parallel processing in the mammalian retina. Nat. Rev. Neurosci. *5*, 1–11.

Wong, R.O.L., and Ghosh, A. (2002). Activity-dependent regulation of dendritic growth and patterning. Nat. Rev. Neurosci. *3*, 803–812.

Wu, G.-Y., Zou, D.J., Rajan, I., and Cline, H. (1999). Dendritic dynamics in vivo change during neuronal maturation. J. Neurosci. *19*, 4472–4483.

Xiao, T., Roeser, T., Staub, W., and Baier, H. (2005). A GFP-based genetic screen reveals mutations that disrupt the architecture of the zebrafish retinotectal projection. Development *132*, 2955–2967.

Xu, H., and Tian, N. (2004). Pathway-specific maturation, visual deprivation, and development of retinal pathway. Neuroscientist *10*, 337–346.

Yamagata, M., Weiner, J.A., and Sanes, J.R. (2002). Sidekicks: synaptic adhesion molecules that promote lamina-specific connectivity in the retina. Cell *110*, 649–660.